Archives of Mechanics • Archiwum Mechaniki Stosowanej • 25, 2, pp. 137–154, Warszawa 1973

Transient thermal stresses in a disc of linearly strain-hardening material

H. ODENÖ (LINKÖPING)

A THIN circular disc of linearly strain hardening material, subjected to an axially symmetric transient temperature field, is treated analytically. All physical properties of the material, except the yield stress, are assumed to be temperature independent. Poisson's ratio is taken to be one half. The material is assumed to obey the Tresca yield criterion and its associated flow rule. The transient temperature field considered, is that ensuing from a rapid increase of the rim surface temperature. The heat conduction equation is solved approximately by the collocation method. The analysis shows, that under certain circumstances, plastic deformation will occur in moving annular regions. Numerical examples are shown, illustrating, at various magnitudes of thermal loading, the influence of a linearly temperature dependent yield stress and the effects of strain hardening.

Rozpatrzono analitycznie zagadnienie cienkiej tarczy okrągłej z materiału wykazującego liniowe wzmocnienie, poddanej działaniu chwilowego pola temperatury. Wszystkie fizykalne własności materiału z wyjątkiem granicy plastyczności przyjęto jako niezależne od temperatury. Współczynnik Poissona założono równy połowie. Materiał podlega warunkom plastyczności Treski i związanego z nim prawa płynięcia. Rozważane chwilowe pole temperatury wynika z szybkiego wzrostu temperatury powierzchniowej. Równanie przewodnictwa ciepła rozwiązano w sposób przybliżony za pomocą metody kolokacji. Analiza wykazała, że przy pewnych warunkach plastyczne deformacje mogą powstać w poruszających się obwodach pierścieniowych. Przykłady numeryczne zilustrowały przy różnych wielkościach termicznego obciążenia wpływ liniowej zależności od temperatury granicy plastyczności oraz efektów wzmocnienia.

Аналитически исследована задача о тонком круглом диске из линейно упрочняющегося материала, подверженном воздействию мгновенного осесимметрического температурного поля. Предполагается, что все физические свойства материала, за исключением предела текучести, не зависят от температуры. Коэффициент Пуассона принят равным половине, материал удовлетворяет условию текучести Треска и ассоциированному с ним закону течения. Рассматриваемое мгновенное температурное поле возникает при внезапном увеличении поверхностей температуры. Уравнение теплопроводности решается приближенным образом по методу коллокации. Даны численные примеры, иллюстрирующие влияние линейной температурной зависимости предела текучести и упрочнения при различных значениях термической нагрузки.

1. Introduction

THERMAL loads on structures are increasingly common in modern engineering. At moderate temperature gradients, the deformations are usually elastic. At higher temperature gradients, and with rising temperatures, however, two effects tend to cause plastic deformations: the thermal stresses increase and the yield stress of most materials decreases with rising temperature.

Many technical applications, subjected to thermal loads, concern structures with complicated shapes. The thermal stress analysis then becomes cumbersome, and numerical

procedures must be introduced at an early stage. However, studies of idealized problems, which are possible to treat analytically, are essential in showing the general features of thermal stress problems. In particular, the influence of different material properties may be investigated in such idealized studies.

In the present paper, the state of stress and strain in a circular disc, subjected to a prescribed temperature history at the rim surface, will be analysed. The transient temperature field appearing will cause plastic flow in moving annular regions, if the temperature change at the rim surface is of sufficient magnitude and rate.

The following behaviour is assumed for the disc material. In the range below a temperature-dependent yield limit, it behaves elastically. Above this limit, the material will begin to deform plastically with a linear rate of strain hardening. The Tresca yield criterion and its associated flow rule will be used, since in this case it offers certain simplifications.

The mechanical properties of a material are, in general, temperature dependent. However, this dependence is more significant for the yield stress than for other properties such as Young's modulus and Poisson's ratio. For an ordinary carbon steel, the relative reduction in yield stress will be more than four times the relative reduction in Young's modulus at a temperature increase from 20° to 250°C. In view of this, the temperature dependence will be disregarded for all material properties except the yield stress.

A considerable number of papers have been published on the problem of plastic flow in cylindrical bodies, subjected to temperature gradients. Most of these investigations concern steady-state temperature fields, materials without strain hardening, and cases in which the yield stress is assumed to be temperature independent. However, in Ref. [1] the effect of strain hardening is considered in thick-walled tubes subjected to internal and external pressures and to steady-state temperature gradients.

Problems in which the temperature field is transient are usually treated by numerical procedures. Refs. [2 and 3] investigate transient heat-treated long solid and hollow circular cylinders of non-strain hardening elasto-plastic material. The latter considers the temperature dependence of the yield stress.

A problem connected with that of the present paper is treated in [4]. A disc of elastic-perfectly plastic material, with all material properties assumed to be temperature independent, is heated by a heat source of circular shape and constant output. During heating there occurs a plastic region near the heat source which, after removal of the source, is absorbed by an unloaded region. For an infinite disc, the stress field is calculated numerically.

In [5] are studied thermal and residual stresses and deformations in a thin ring disc, initially at uniform temperature. The temperature at the inner edge of the ring is raised to a constant value. The outer edge is insulated and there is heat transfer from the lateral surfaces to the surrounding medium. The actual temperature field is replaced by a simple approximation and the problem is solved for an elastic-perfectly plastic disc material using a temperature dependent yield stress. Some numerical calculations are carried out in relation to case studies and design rules are given.

Various aspects of the present problem have been treated in earlier papers by the present author. In [6], dealing with the method of dismantling the ring in a shrink-fit by heating the outer rim surface, the material was assumed to be elastic-perfectly plastic and

the yield stress to be independent of the temperature. Such dependence was included in the analysis carried out in [7].

Thermal stresses in elasto-plastic cylindrical bodies are treated in general form in a number of monographs. Hence [8–10] may be regarded as general references on the present subject.

Exact solutions of transient temperature fields usually result in rather cumbersome mathematical expressions. Good estimates may often be found by approximate methods, which essentially simplify the computations. The numerical calculations may then be carried out on small computers, using simple computer programs. Such an approximate temperature field solution will be applied in the present investigation.

2. Notation

A, B, D, F, K functions of the time,
E Young's modulus,
G shear modulus,
$T(x,t)$ temperature,
T_k total temperature increase,
$\overline{T}(x,t) = (1/x^2)\int Tx\,dx$,
b disc radius,
e_i deviatoric strain components,
f, g, h, j, k functions of the radius,
i index: $i = r, \theta, z$,
r, θ, z cylindrical coordinates,
s_i deviatoric stress components,
t time,
t_1, t_2, t_3, t_4 times denoting the start or end of an elastic or plastic region,
$t^*(x_2)$ time corresponding to $x = x_2$,
u dimensionless radial displacement,
$x = r/b$ dimensionless radial coordinate,
x_1, x_2, x_3 radii defined in Fig. 2,
$x_{1\infty}, x_{3\infty}$ ultimate values of x_1 and x_3,
α coefficient of thermal expansion,
β parameter introduced in (4.1),
δ linear strain-hardening parameter,
ε_i strain components,
ε_p effective plastic strain,
$\varkappa$ thermal diffusivity,
ϱ yield stress reduction,
σ_i stress components,
$\overline{\sigma} = (\sigma_r+\sigma_\theta+\sigma_z)/3$ mean stress,
σ_e effective stress,
σ_s initial yield stress,
$\tau = b^2/4\varkappa$.

Superscripts E and P denote elastic and plastic quantities, respectively.

3. General stress and strain formulations

Consider a solid disc with radius b, subjected to a known axially symmetric transient temperature field, which does not vary throughout the thickness. Then the principal axes

of the stress and strain fields at all points of the disc coincide with the directions of the cylindrical coordinates r, θ, z. It is convenient to introduce a dimensionless radius, $x = r/b$.

In order to simplify the analysis, Poisson's ratio is taken as 0.5. This means that the material is elastically (as well as plastically) incompressible and volume changes are due solely to temperature variations. Hence the mechanical incompressibility relation could be written as:

$$\frac{\partial u}{\partial x} + \frac{u}{x} + \varepsilon_z = 3\alpha T, \tag{3.1}$$

where u is the radial displacement divided by b. From integration of (3.1) follows, considering that the axial strain ε_z is a function of both time and radius,

$$u = \frac{3\alpha}{x}\int Tx\,dx - \frac{1}{x}\int \varepsilon_z x\,dx + \frac{B(t)}{x}.$$

The deviatoric strain rates then are:

$$\begin{aligned} \dot{e}_r &= 2\alpha\dot{T} - 3\alpha\dot{\overline{T}} - \dot{\varepsilon}_z + \frac{1}{x^2}\int \dot{\varepsilon}_z x\,dx - \frac{\dot{B}}{x^2}, \\ \dot{e}_\theta &= -\alpha\dot{T} + 3\alpha\dot{\overline{T}} - \frac{1}{x^2}\int \dot{\varepsilon}_z x\,dx + \frac{\dot{B}}{x^2}, \\ \dot{e}_z &= -\alpha\dot{T} + \dot{\varepsilon}_z. \end{aligned} \tag{3.2}$$

In (3.2), the notation $\overline{T} = (1/x^2)\int Tx\,dx$ has been introduced. Poisson's ratio equals 0.5 and consequently the Eqs. (3.2) are valid for elastic as well as plastic states.

3.1. Elastic state

The equation of equilibrium and the relation between deviatoric elastic strain components, e_i^E, and deviatoric stress components, s_i – viz.

$$\frac{\partial \sigma_r}{\partial x} + \frac{\sigma_r - \sigma_\theta}{x} = 0, \quad s_i = 2Ge_i^E, \quad i = r, \theta, z \tag{3.3}$$

are used to find the stress and strain fields in those parts of the disc where the state is elastic. From the procedure adopted in [7], the stresses and strains may be written as

$$\begin{aligned} \sigma_r &= E\left[-\alpha\overline{T} - 2D(t) - \frac{2}{3}\frac{B(t)}{x^2} + f_r(x)\right], \\ \sigma_\theta &= E\left[-\alpha T + \alpha\overline{T} - 2D(t) + \frac{2}{3}\frac{B(t)}{x^2} + f_\theta(x)\right], \end{aligned} \tag{3.4}$$

$$\begin{aligned} \varepsilon_r &= \frac{3\alpha}{2}T - \frac{3\alpha}{2}\overline{T} - D(t) - \frac{B(t)}{x^2} + g_r(x), \\ \varepsilon_\theta &= \frac{3\alpha}{2}\overline{T} - D(t) + \frac{B(t)}{x^2} + g_\theta(x), \\ \varepsilon_z &= \frac{3\alpha}{2}T + 2D(t) + g_z(x), \end{aligned} \tag{3.5}$$

where $B(t)$, $D(t)$, $f_i(x)$ and $g_i(x)$ are as yet unknown functions.

3.2. Plastic state

In the plastic range, linear strain-hardening of the material will be assumed, cf. Fig. 3. For the physical properties of the material, except for the yield stress, the temperature dependence will be disregarded. The Tresca yield criterion with associated flow rule will be used.

For the state of stress studied in the present paper, the effective stress takes the form $\sigma_e = \sigma_r - \sigma_\theta$ during loading periods — i.e., when plastic deformations are due to increasing temperature gradients, and $\sigma_e = \sigma_\theta - \sigma_r$ during periods of reversed plastic flow. According to the flow rule associated with the Tresca criterion, the plastic strain increments could be written as:

$$d\varepsilon_\theta^P = -d\varepsilon_r^P, \quad d\varepsilon_z^P = 0. \tag{3.6}$$

There are two methods generally applied to obtain the effective plastic strain increment, $d\varepsilon_p$, and in this case they differ by a constant $2/\sqrt{3}$, cf. [10]. In the following analysis, the effective plastic strain increment is defined as

$$d\varepsilon_p = |d\varepsilon_r^P|. \tag{3.7}$$

The stress-strain relation will take different forms in different regions, depending on the direction of loading. In the loading period

$$\varepsilon_p = \frac{1-\delta}{\delta E}(\sigma_e - \sigma_s), \tag{3.8}$$

where the strain-hardening parameter δ is defined as the ratio of the slope of strain-hardening part of the one-dimensional stress-strain relation to the elastic modulus.

Using (3.7), (3.8), and the fact that the condition of loading is equivalent to $d\varepsilon_r^P \geqslant 0$, we obtain

$$\dot{\sigma}_r - \dot{\sigma}_\theta = \dot{\sigma}_s + \frac{\delta E}{1-\delta}\dot{\varepsilon}_r^P. \tag{3.9}$$

Integration of the equilibrium Eq. (3.3), after substitution of (3.9), leads to

$$\begin{aligned} \dot{\sigma}_r &= -\int \frac{\dot{\sigma}_s}{x}dx - \frac{\delta E}{1-\delta}\int \frac{\dot{\varepsilon}_r^P}{x}dx + \dot{F}(t), \\ \dot{\sigma}_\theta &= -\int \frac{\dot{\sigma}_s}{x}dx - \dot{\sigma}_s - \frac{\delta E}{1-\delta}\int \frac{\dot{\varepsilon}_r^P}{x}dx - \frac{\delta E}{1-\delta}\dot{\varepsilon}_r^P + \dot{F}(t), \end{aligned} \tag{3.10}$$

where $\dot{F}(t)$ is an as yet unknown function of time.

In order to find formulations for stresses and strains, similar to those in the elastic range, the two rates $\dot{\varepsilon}_r^P$ and $\dot{\varepsilon}_z$ must be determined. From (3.6) follows $\dot{\varepsilon}_z^P = 0$, i.e. $\dot{\varepsilon}_z = \dot{\varepsilon}_z^E$. Then the second of the relations (3.3) holds for $\dot{\varepsilon}_z$, and together with the condition of zero stresses in the axial direction there follows:

$$\dot{\bar{\sigma}} = 2G(\alpha\dot{T} - \dot{\varepsilon}_z).$$

Using the Eqs. (3.10) to obtain $\dot{\bar{\sigma}}$ it is found that

$$\dot{\varepsilon}_z = \alpha\dot{T} + \frac{1}{6G}\left(2\int \frac{\dot{\sigma}_s}{x}dx + \dot{\sigma}_s\right) + \frac{\delta}{2(1-\delta)}\left(2\int \frac{\dot{\varepsilon}_r^P}{x}dx + \dot{\varepsilon}_r^P\right) - \frac{\dot{F}(t)}{3G}. \tag{3.11}$$

The plastic strain rate, $\dot{\varepsilon}_r^P$, may be written as $\dot{e}_r - \dot{e}_r^E$, where $\dot{e}_r$ follows from (3.2) and $\dot{e}_r^E$ from (3.3), (3.10). It is found after some calculation, using (3.11), that

$$\dot{\varepsilon}_r^P = (1-\delta)\left[\alpha\dot{T} - 2\alpha\dot{\bar{T}} - \frac{\dot{\sigma}_s}{3G} + \frac{\dot{K}(t)}{x^2}\right], \tag{3.12}$$

where $\dot{K}(t)$ is an as yet unknown function of time. Substitution of (3.12) into (3.11) yields:

$$\dot{\varepsilon}_z = \alpha\dot{T} + \frac{\delta}{2}\alpha\dot{T} + \frac{1-\delta}{6G}\left(2\int\frac{\dot{\sigma}_s}{x}dx + \dot{\sigma}_s\right) - \frac{\dot{F}(t)}{3G}. \tag{3.13}$$

It is now possible to formulate general stress and strain equations in a plastic region, where $\sigma_e = \sigma_r - \sigma_\theta$. The stresses are found by integration of (3.10), after substitution of (3.12), and the strains by integration of (3.2), where $\dot{\varepsilon}_z$ is given by (3.13). There results:

$$\begin{aligned}
\sigma_r &= -(1-\delta)\int\frac{\sigma_s}{x}dx - \delta\alpha E\bar{T} + \frac{\delta E K(t)}{2x^2} + F(t) + k_r(x), \\
\sigma_\theta &= -(1-\delta)\left(\int\frac{\sigma_s}{x}dx + \sigma_s\right) - \delta\alpha E(T-\bar{T}) - \frac{\delta E K(t)}{2x^2} + F(t) + k_\theta(x),
\end{aligned} \tag{3.14}$$

$$\begin{aligned}
\varepsilon_r &= \left(2-\frac{\delta}{2}\right)\alpha(T-\bar{T}) - \frac{1-\delta}{2E}\left(\int\frac{\sigma_s}{x}dx + \sigma_s\right) + \left(1-\frac{\delta}{4}\right)\frac{K(t)}{x^2} + \frac{F(t)}{2E} + h_r(x), \\
\varepsilon_\theta &= \left(2-\frac{\delta}{2}\right)\alpha\bar{T} - \frac{1-\delta}{2E}\int\frac{\sigma_s}{x}dx - \left(1-\frac{\delta}{4}\right)\frac{K(t)}{x^2} + \frac{F(t)}{2E} + h_\theta(x), \\
\varepsilon_z &= \left(1+\frac{\delta}{2}\right)\alpha T + \frac{1-\delta}{E}\int\frac{\sigma_s}{x}dx + \frac{1-\delta}{2E}\sigma_s - \frac{F(t)}{E} + h_z(x),
\end{aligned} \tag{3.15}$$

where k_r, k_θ, h_r, h_θ and h_z are as yet unknown functions of x.

The Eqs. (3.4), (3.5) and (3.14), (3.15), valid in elastic and plastic regions respectively, involve a number of unknown functions. The time dependent functions, B, D, F, K, will be determined from either boundary or continuity conditions. The functions which depend only on the radius, f, g, h, k, will be different from zero if there exists a residual strain field or if any external forces are acting on the disc.

4. Temperature field

The following type of thermal loading will be considered. The two plane faces of the disc are insulated so as to prevent any thermal losses. The rim surface is subjected to a prescribed temperature history, as indicated in Fig. 1.

At $t = 0$, a rapid increase of the rim surface temperature starts. The thermal load history is given by the following function,

$$T(1, t) = T_k[1 - \exp(-\beta t)], \tag{4.1}$$

where βT_k is the initial rate of temperature change.

The temperature field is assumed to be axially uniform and circularly symmetric. The solution of the heat conduction equation results in a series, in which products of the Bessel

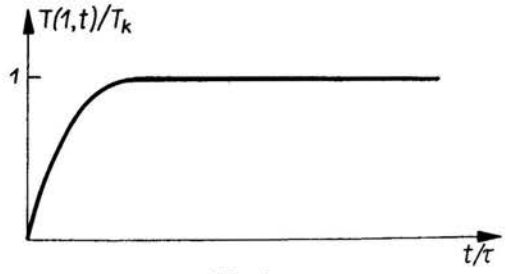

FIG. 1.

function J_0 (argument x) and the exponential function (argument t) are the elements. For the purpose of this paper, an approximate solution will be sufficient. The Bessel function J_0 contains only even powers of x and, therefore, the following approximation of the temperature field has been used:

$$T(x, t) = A_0(t) - A_2(t)\,(1-x^2) - A_4(t)\,(1-x^4).$$

The three functions A_0, A_2, A_4 are determined by the boundary condition (4.1) and by the method of collocation, cf. [11], with collocations at $x = 0$ and $x = 1/\sqrt{2}$. This approximate temperature field solution, applied to the case of elastic stresses only, is discussed in [12]. An exact elastic solution for the case $\beta = \infty$ — that is, an instantaneous temperature change at $x = 1$ — is presented in [13]. The highest numerical values of stress in the disc are obtained at the rim. From a comparison, carried out in [12], of the exact and approximate solutions, Table 1 shows the ratio of approximately and exactly calculated values on $\sigma_\theta(1, t)$, where $\tau = b^2/4\varkappa$.

Table 1

t/τ	$\frac{\sigma_\theta(1,t)\ \text{approx}}{\sigma_\theta(1,t)\ \text{exact}}$	$\frac{\sigma_\theta(1,t)\ \text{exact}}{\alpha E T_k}$
0	0.83	−1
0.02	0.93	−0.87
0.05	0.99	−0.77
0.10	1.01	−0.68
0.50	1.00	−0.33
1.0	1.00	−0.16

The approximation cannot reproduce the discontinuous temperature field at $t = 0$ and, consequently, the error shows its maximum there. However, the error rapidly decreases. In the numerical examples, subsequently shown, the parameter β is taken to be $50/\tau$ and it should be noted that the error may be expected to drop at finite values of β.

5. Analysis of transient fields

The stress and strain fields caused by the thermal loading (4.1) on the disc will now be investigated. First, it may be of some interest to describe the pattern of elastic and plastic regions occurring during transient thermal loading. The subsequent analysis will

show that four different cases can be distinguished. Hence the analysis will be divided into four time intervals as follows:

I $$0 \leqslant t \leqslant t_1$$

The state of stress is elastic at every point in the disc.

II $$t_1 < t \leqslant t_2$$

At $t = t_1$, yielding starts at the rim of the disc and then spreads inwards. Hence in this interval the disc is divided into two regions, one elastic at the core of the disc and one plastic at the rim. The boundary radius between the two regions is a function of time, denoted by $x = x_1(t)$.

III $$t_2 < t \leqslant t_3$$

In this interval, a new elastic region appears at the rim, where unloading starts at $t = t_2$. The plastic region, surrounded by the two elastic regions, continues to move inwards. The boundary radius between the plastic region and the outer elastic region is denoted by $x = x_2(t)$.

IV $$t_3 < t$$

During the unloading course, reversed plastic flow starts at the rim at $t = t_3$. Hence the disc is divided into four regions, where the stress state is elastic, plastic, elastic and

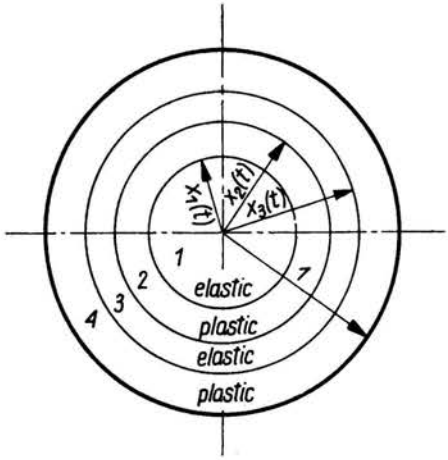

FIG. 2.

plastic, counting from the centre of the disc, cf. Fig. 2. The boundary radius separating the two latter regions is denoted by $x = x_3(t)$. The inner plastic region vanishes after a certain time, which may be greater or lesser than t_3.

5.1. Time interval I

The state of stress will be elastic throughout the disc during the first phase of thermal loading. The stress and strain fields are given by the Eqs. (3.4), (3.5). The disc is supposed to be stress and strain free at $t = 0$ and, therefore, the functions $f_i(x)$, $g_i(x)$ will be zero.

The strain components must be finite at $x = 0$, which requires $B(t) = 0$, and the boundary condition,

$$\sigma_r(1, t) = 0, \tag{5.1}$$

results in $D(t) = -\alpha\bar{T}(1, t)/2$. The stresses are then obtained as

$$\sigma_r = \alpha E[\bar{T}(1, t) - \bar{T}(x, t)],$$
$$\sigma_\theta = \alpha E[-T + \bar{T}(1, t) + \bar{T}(x, t)].$$

The effective stress at $x = 1$, $\sigma_e = \sigma_r - \sigma_\theta = \alpha E[T(1, t) - 2\bar{T}(1, t)]$ increases with time and reaches the yield stress at time $t = t_1$.

5.2. Time interval II

After the time $t = t_1$, a plastic region grows inwards the disc. At time t, initial yielding will be reached at the radius denoted by $x = x_1(t)$. In the subsequent analysis, the elastic and plastic regions are indicated by the indices 1 and 2, respectively. The stress and strain fields are given by the Eqs. (3.4), (3.5) and (3.14), (3.15). For the same reason as in the previous section, the radial functions (f, g, k, h) and the function $B_1(t)$ will be zero.

The yield stress depends on the temperature, but $T = T(x, t)$ and hence $\sigma_s = \sigma_s(T) = \sigma_s(x, t)$. In the elastic region, the criterion of initial yielding should be reached at $x = x_1$ — that is,

$$\sigma_{r1}(x_1, t) - \sigma_{\theta 1}(x_1, t) = \alpha E[T(x_1, t) - 2\bar{T}(x_1, t)] = \sigma_s(x_1, t). \tag{5.2}$$

From the Eq. (5.2), the boundary radius $x_1(t)$ may be calculated. The three remaining functions — viz. D_1, F_2, K_2 — are determined from (5.1) and from the continuity conditions:

$$\sigma_{r1}(x_1, t) = \sigma_{r2}(x_1, t),$$
$$\varepsilon_{\theta 1}(x_1, t) = \varepsilon_{\theta 2}(x_1, t). \tag{5.3}$$

In the elastic region $(0 \leqslant x < x_1)$, the stresses are given by

$$\sigma_{r1} = \alpha E[(1-\delta)\bar{T}(x_1, t) + \delta\bar{T}(1, t) - \bar{T}(x, t)] + (1-\delta)\int_{x_1}^{1} \frac{\sigma_s}{x} dx,$$

$$\sigma_{\theta 1} = \alpha E[-T + (1-\delta)\bar{T}(x_1, t) + \delta\bar{T}(1, t) + \bar{T}(x, t)] + (1-\delta)\int_{x_1}^{1} \frac{\sigma_s}{x} dx,$$

and in the plastic region $(x_1 \leqslant x \leqslant 1)$, by

$$\sigma_{r2} = \delta\alpha E[\bar{T}(1, t) - \bar{T}(x, t)] + (1-\delta)\int_{x}^{1} \frac{\sigma_s}{y} dy,$$

$$\sigma_{\theta 2} = \delta\alpha E[-T + \bar{T}(1, t) + \bar{T}(x, t)] + (1-\delta)\left(\int_{x}^{1} \frac{\sigma_s}{y} dy - \sigma_s\right).$$

In region 2, the plastic strain rate is

$$\dot{\varepsilon}_{r2}^{P} = (1-\delta)\left[\alpha\dot{T}-2\alpha\dot{\bar{T}}(x,t)-\frac{\dot{\sigma}_s}{E}\right],$$

which follows from (3.12) and the calculated function $K(t)$. In the plastic region, $\dot{\varepsilon}_{r2}^{P}$ should be non-negative and as the rate changes sign, unloading takes place. This will happen, starting at $x = 1$, for a certain time $t = t_2$, and a new elastic region appears.

5.3. Time interval III

In this time interval, the plastic region will be surrounded by two elastic regions. The outer elastic region, denoted by the index 3, expands inwards and has at time t reached the radius $x_2(t)$. Among the functions to be determined, it is easily found that B_1, f_1, g_1, k_2, h_2 are all zero. The boundary radius $x_1(t)$ is obtained from (5.2). From one of the conditions (5.3) K_2 is found to be zero. The boundary radius $x_2(t)$ is the location, where the plastic strain rate changes sign and hence, by means of (3.12), may be obtained from,

$$\left[\alpha\dot{T}(x,t)-2\alpha\dot{\bar{T}}(x,t)-\frac{\dot{\sigma}_s(x,t)}{E}\right]_{x=x_2} = 0. \tag{5.4}$$

At $x = x_2$, the plastic strain components are "frozen", since the state of stress changes from plastic to elastic. Hence a residual plastic strain field appears in region 3 with the components:

$$\varepsilon_{r3}^{P} = -\varepsilon_{\theta 3}^{P} = j(x), \quad \varepsilon_{z3}^{P} = 0, \tag{5.5}$$

and from the Eq. (3.12), where $K(t) = 0$, follows

$$j(x_2) = (1-\delta)\left[\alpha T(x_2,t^*)-2\alpha\bar{T}(x_2,t^*)-\frac{1}{E}\sigma_s(x_2,t^*)\right],$$

where $t^* = t^*(x_2)$ is calculated from (5.4).

The five radial functions in region 3 ($f_{r3}, f_{\theta 3}, g_{r3}, g_{\theta 3}, g_{z3}$) are determined from the equation of equilibrium (3.3), the equation of compatibility

$$\frac{\partial\varepsilon_{\theta 3}}{\partial x}+\frac{\varepsilon_{\theta 3}-e_{r3}}{x} = 0, \tag{5.6}$$

and the elasticity relation (3.3), where the elastic parts of the strain components are obtained by subtracting the plastic components (5.5) and the thermal components αT from the total components in (3.5). Elimination of all functions but f_{r3} leads to a differential equation,

$$\frac{d^2f_{r3}}{dx^2}+\frac{3}{x}\frac{df_{r3}}{dx} = \frac{1}{x}\frac{dj}{dx}+\frac{2}{x^2}j. \tag{5.7}$$

The solution of (5.7), where the homogeneous part k_1+k_2/x^2 may be included in D_3 and B_3 respectively, results in the following set of radial functions:

$$\begin{aligned} &f_{r3} = \int\frac{j}{x}dx, \quad f_{\theta 3} = j+\int\frac{j}{x}dx, \\ &g_{r3} = \frac{1}{2}\left(j+\int\frac{j}{x}dx\right), \quad g_{\theta 3} = \frac{1}{2}\int\frac{j}{x}dx, \quad g_{z3} = -\frac{1}{2}\left(j+2\int\frac{j}{x}dx\right). \end{aligned} \tag{5.8}$$

The remaining time functions D_1, F_2, B_3, D_3 are obtained from (5.1), one of the conditions (5.3) and the two continuity conditions at $x = x_2$;

$$\sigma_{r2}(x_2, t) = \sigma_{r3}(x_2, t), \quad \varepsilon_{\theta 2}(x_2, t) = \varepsilon_{\theta 3}(x_2, t).$$

There results

$$D_1 = \frac{\alpha}{2}[-\bar{T}(1, t)+(1-\delta)\bar{T}(x_2, t)-(1-\delta)\bar{T}(x_1, t)]-\frac{1-\delta}{2E}\int_{x_1}^{x_2}\frac{\sigma_s}{x}dx+\frac{1}{2}\int_{x_2}^{1}\frac{j}{x}$$

$$F_2 = \alpha E[\bar{T}(1, t)-(1-\delta)\bar{T}(x_2, t)]+(1-\delta)\int^{x_2}\frac{\sigma_s}{x}dx-E\int_{x_2}^{1}\frac{j}{x}dx,$$

$$B_3 = 0, \quad D_3 = -\frac{\alpha}{2}\bar{T}(1, t)+\frac{1}{2}\int^{1}\frac{j}{x}dx.$$

Then all unknown functions are found and the complete states of stress and strain are known in this time interval. In the outer elastic region, where unloading takes place, reversed plastic flow may occur, starting at $x = 1$.

5.4. Time interval IV

Reversed plastic flow is assumed to start when the effective stress, now $\sigma_e = \sigma_\theta - \sigma_r$, reaches the value $\sigma_s(T)$ — that is, the Bauschinger effect is disregarded. Fig. 3 illustrates the proposed material model, which is more fully discussed in [14].

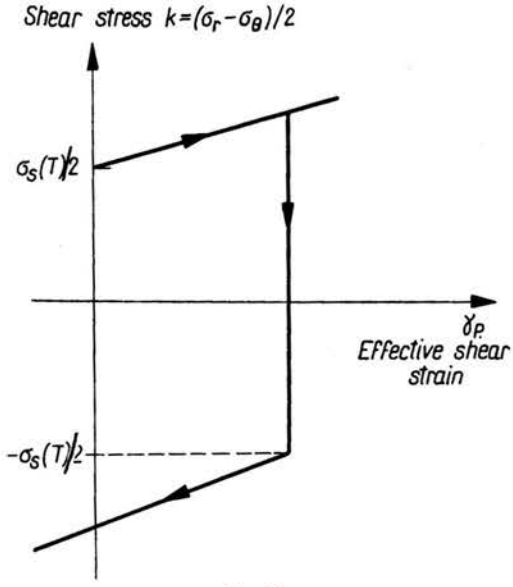

FIG. 3.

In the region of reversed plastic flow, denoted by the index 4, it is easily shown that general stress and strain field formulations are obtained by replacing σ_s by $-\sigma_s$ in the Eqs.

(3.14) and (3.15). The effective plastic strain increment in region 4 will be $d\varepsilon_p = d\varepsilon_\theta^P = -d\varepsilon_r^P \geqslant 0$. Recalling the relation (3.8) between ε_p and σ_e, and taking into account that $\varepsilon_r^P = j(x)$ when $\sigma_e = \sigma_s$, it is found that

$$\varepsilon_r^P = -\varepsilon_\theta^P = -\frac{1-\delta}{\delta E}(\sigma_e - \sigma_s) + j(x), \qquad \varepsilon_z^P = 0. \tag{5.9}$$

The plastic strain components may also be evaluated from general stress and strain formulations. The elastic strain components are calculated from the elasticity relation in (3.3). Subtracting the elastic and thermal parts from the total components in (3.15), where σ_s should be changed to $-\sigma_s$, the plastic parts are found. Substituting these parts into (5.9), three relations between the five functions $k_{r4}, k_{\theta 4}, h_{r4}, h_{\theta 4}, h_{z4}$ are established. The two additional relations to be used are the equations of equilibrium (3.3) and compatibility (5.6). Since the above-mentioned relations are essentially the same as those leading to the Eq. (5.7), it is not surprising to find that in this case a similar differential equation is obtained. The five functions are $k_{i4} = \delta E f_{i3}$ and $h_{i4} = \delta g_{i3}$, where f_{i3} and g_{i3} are given by (5.8).

The radial functions in region 3, namely f_3 and g_3, are found in a manner similar to that in the previous interval, to be the same as in (5.8). During this time interval, the disc is divided into four regions, cf. Fig. 2. The radius, where reversed yielding starts at time t, is denoted by $x = x_3(t)$. The three boundary radii x_1, x_2 and x_3 are obtained from (5.2), (5.4) and

$$\sigma_{\theta 3}(x_3, t) - \sigma_{r3}(x_3, t) = Ej(x_3) - \alpha E[T(x_3, t) - 2\bar{T}(x_3, t)] = \sigma_s(x_3, t).$$

The time functions are determined by boundary and continuity conditions and are found to be:

$$B_1 = K_2 = B_3 = K_4 = 0,$$

$$D_1 = \frac{(1-\delta)\alpha}{2}[-\bar{T}(x_3, t) + \bar{T}(x_2, t) - \bar{T}(x_1, t)] - \frac{\delta}{2}\left[\alpha\bar{T}(1, t - \int_{x_3}^{1} \frac{j}{x} dx\right]$$

$$- \frac{1-\delta}{2E}\left(\int_{x_1}^{x_2} \frac{\sigma_s}{x} dx - \int_{x_3}^{1} \frac{\sigma_s}{x} dx\right) + \frac{1}{2}\int_{x_2}^{x_3} \frac{j}{x} dx,$$

$$F_2 = (1-\delta)\alpha E[\bar{T}(x_3, t) - \bar{T}(x_2, t)] + \delta E\left[\alpha\bar{T}(1, t) - \int_{x_3}^{1} \frac{j}{x}\, x\right]$$

$$+ (1-\delta)\left(\int_{x_2}^{x_3} \frac{\sigma_s}{x} dx - \int_{x_3}^{1} \frac{\sigma_s}{x} dx\right) - E\int_{x_2}^{x_3} \frac{j}{x} dx,$$

$$D_3 = -\frac{(1-\delta)\alpha}{2}\bar{T}(x_3, t) - \frac{\delta}{2}\left[\alpha\bar{T}(1, t) - \int_{x_3}^{1} \frac{j}{x} dx\right] + \frac{1-\delta}{2E}\int_{x_3}^{1} \frac{\sigma_s}{x} dx + \frac{1}{2}\int_{x_3}^{x_3} \frac{j}{x} dx,$$

$$F_4 = \delta\alpha E\bar{T}(1, t) - (1-\delta)\int_{x_3}^{1} \frac{\sigma_s}{x} dx - \delta E\int_{x_3}^{1} \frac{j}{x} dx.$$

The stress and strain fields are then known at every point of the disc during this time interval. The inner plastic region — i.e. region 2 — shrinks to zero after a certain time $t = t_4$, when $x_1(t_4) = x_2(t_4)$. This may happen either in this interval ($t_4 > t_3$) or in the previous interval ($t_4 < t_3$).

After a long time, the temperature in the entire disc reaches the value $T(x, t) = T_k$, and a residual state of stress is left in the disc. The tangential component may be written as,

$$\sigma_\theta(x, \infty) = (1-\delta)\sigma_s(T_k)\ln x_{3\infty} - E\left(\int_{x_{1\infty}}^{x_{3\infty}} \frac{j}{x}dx + \delta\int_{x_{3\infty}}^{1}\frac{j}{x}dx\right), \quad 0 \leqslant x \leqslant x_{1\infty},$$

$$(1-\delta)\sigma_s(T_k)\ln x_{3\infty} + E\left(j - \int_{x}^{x_{3\infty}}\frac{j}{y}dy - \delta\int_{x_{3\infty}}^{1}\frac{j}{x}dx\right), \quad x_{1\infty} < x \leqslant x_{3\infty}, \tag{5.10}$$

$$(1-\delta)\sigma_s(T_k)(1+\ln x) + \delta E\left(j - \int_{x}^{1}\frac{j}{y}dy\right), \quad x_{3\infty} < x \leqslant 1,$$

where $x_{1\infty}$ and $x_{3\infty}$ denote the ultimate values of $x_1(t) = x_2(t)$ and $x_3(t)$, respectively. The integral in (5.10) may be written as

$$\int \frac{j}{x}dx = (1-\delta)\left[\alpha\bar{T}(x, t^*) - \frac{1}{E}\int\frac{\sigma_s(x, t^*)}{x}dx\right].$$

6. Numerical calculations

Some samples from numerical calculations will be given to illustrate the influence of different parameters. In the calculations, the parameter β in (4.1) is given the value of $50/\tau$ which means, in relation to the rate at which the temperature propagates into the disc, an almost instantaneous temperature change at $x = 1$.

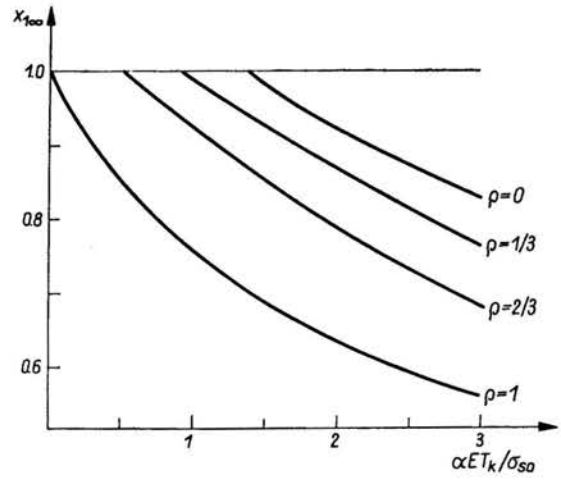

FIG. 4.

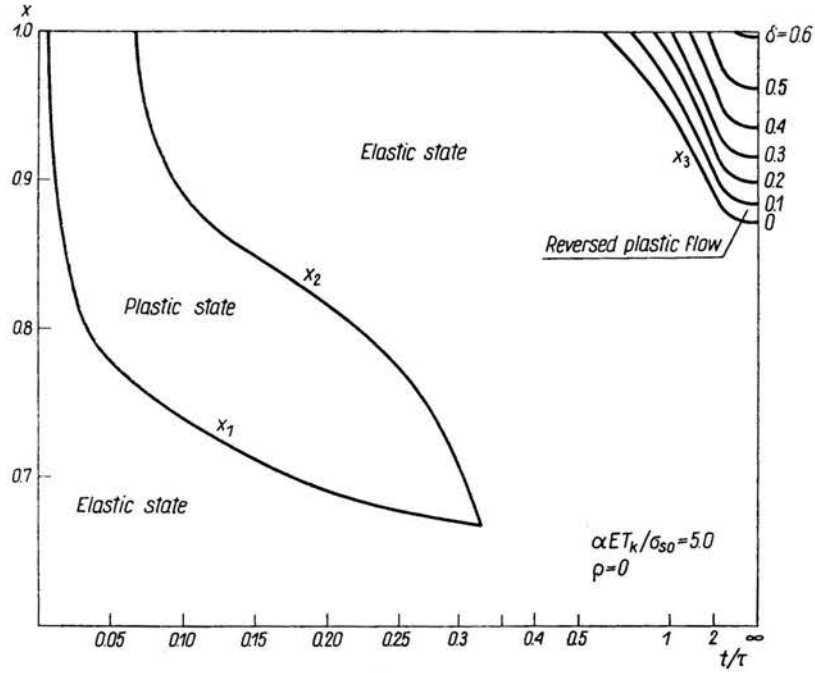

FIG. 5.

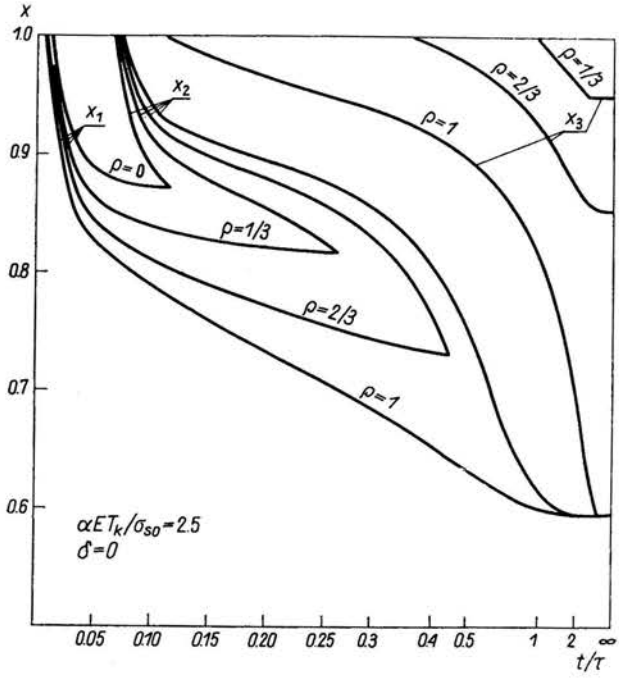

FIG. 6.

In the analysis, the initial yield stress σ_s has been assumed to vary with the temperature. For many materials, this temperature dependence may be considered as linear and therefore the yield stress can be written as

$$\sigma_s = \sigma_{s0}\left(1 - \varrho \frac{T(x,t)}{T_k}\right),$$

where σ_{s0} is the initial yield stress at $T = 0$ and ϱ is the relative reduction in yield stress at the temperature change T_k. It should be noted that ϱ normally depends on the value of T_k.

Figure 4 shows the ultimate value of x_1 — that is, the depth to which the plastic flow penetrates in the disc, as a function of the dimensionless thermal load $\alpha E T_k/\sigma_{s0}$ and the yield stress reduction parameter ϱ. The penetration depth is independent of the strain hardening parameter δ, which is due to the use of the Tresca yield criterion.

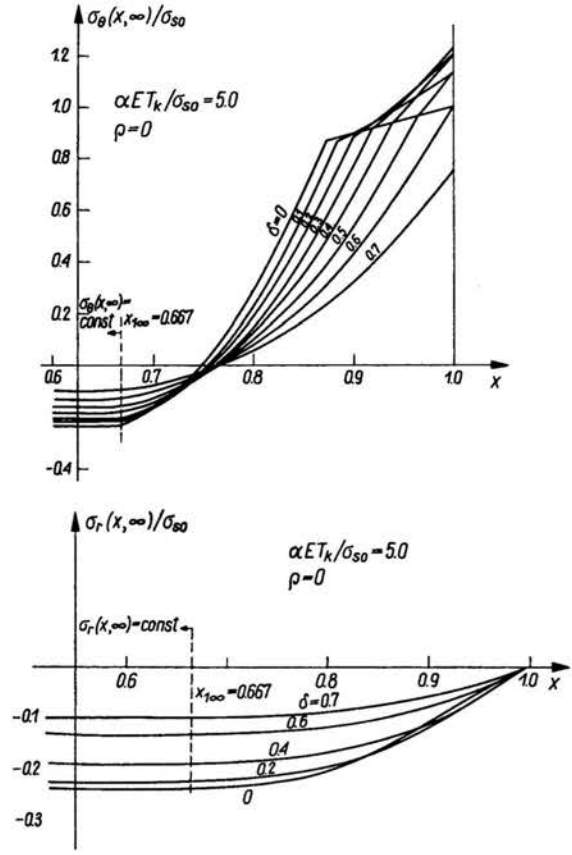

FIG. 7.

By plotting the boundary radii x_1, x_2, x_3 as functions of the time, an illustrative representation of the elastic-plastic pattern in the disc is obtained. Figure 5 shows such a plot for the thermal load $\alpha E T_k/\sigma_{s0} = 5.0$ and $\varrho = 0$ — i.e. no reduction in the yield stress. The strain hardening parameter δ is varied in steps of 0.1 and it is seen from the

plot that this parameter affects the region of reversed plastic flow (x_3) but leaves x_1 and x_2 unaffected. This is in agreement with the previous analysis. For $\delta > 0.61$, no reversed plastic flow takes place.

In Fig. 6, a similar plot is shown for $\alpha E T_k/\sigma_{s0} = 2.5$, $\delta = 0$ and with the values 0, 1/3, 2/3, 1 on the yield stress reduction parameter ϱ. It is obvious that the temperature dependence of the yield stress markedly affects the plastic behaviour in the disc.

It may be of some interest to study the temperature changes corresponding to the dimensionless thermal loads $\alpha E T_k/\sigma_{s0} = 2.5$ and 5.0. For an ordinary carbon steel, starting from a temperature of 20°C, the two values correspond to temperature increases of about 250°C and 500°C, respectively. The relative reduction in yield stress will be of order 0.35 and 0.65, respectively.

Figure 7 shows the residual stress state for $\alpha E T_k/\sigma_{s0} = 5.0$ and $\varrho = 0$. As in Fig. 5, the strain hardening parameter δ is varied in steps of 0.1. Note, that for $x < x_{1\infty} = 0.667$ the stresses are constant. The temperature dependence of the yield stress has, naturally,

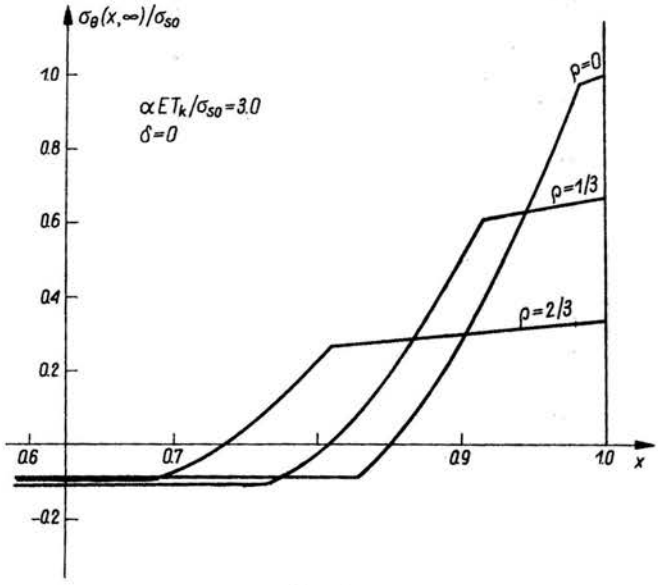

FIG. 8.

a strong influence on the residual state. This is illustrated in Fig. 8, where the residual stress component $\sigma_\theta(x, \infty)$ is plotted for various values of ϱ. The thermal load is taken to be $\alpha E T_k/\sigma_{s0} = 3.0$ and $\delta = 0$ — i.e. there is no strain-hardening. The radial stress component $\sigma_r(x, \infty)$ is omitted, since here the differences, for different values of ϱ, are negligible.

7. Discussion

In [7], the present disc problem is investigated for a material which does not strain harden ($\delta = 0$). The present paper shows that, for linear strain-hardening, a set of terms which all contain the strain-hardening parameter δ, are added to the stress and strain

field equations. However, a of linear strain-hardening involves a moderate increase in the computational work. For strain hardening which cannot be approximated as linear, analytical difficulties appear. Generally, a purely numerical procedure must be applied, cf. [10]. The present investigation may be modified to include non-linear strain-hardening, which can be considered as piece-wise linear. However, the modification markedly increases the computational work and it may therefore be more practical to apply a straightforward numerical procedure.

It should be noted that for thermal loads of the magnitude used in the numerical examples, the plastic parts of the strain components are of the same order as the elastic parts. This means that for practical use the linear approximation of the strain hardening is usually quite sufficient.

The temperature dependence of the yield stress has an important influence on the plastic penetration depth as well as on the reversed plastic flow and the residual stress state. This influence seems, at least for ordinary materials, to be more important than the effects of strain hardening.

It should be pointed out that for reversed plastic flow the treatment in the present investigation is somewhat simplified. The proposed model in Fig. 3 may be too simple for many materials. In particular might the influence of temperature changes on the reversed yield stress be difficult to establish properly.

The temperature levels considered in this study are such that creep deformations occur. However, here the thermal course takes place during a relatively short time and creep may be neglected.

Acknowledgement

The author is indebted to Professor B. STORÅKERS for valuable discussion and positive criticism of this paper.

References

1. D. R. BLAND, *Elasto-plastic thick-walled tubes of work-hardening material, subject to internal and external pressures and to temperature gradients*, J. Mech. Phys. Solids, 4, 209–229, 1956.
2. J. H. WEINER and J. V. HUDDLESTON, *Transient and residual stresses in heat-treated cylinder*, J. Appl. Mech., **26**, 31–39, 1959.
3. H. G. LANDAU and E. E. ZWICKY, *Transient and residual thermal stresses in an elastic-plastic cylinder*, J. Appl. Mech., **27**, 481–488, 1960.
4. U. GAMER, *Ein radialsymmetrischer Wärmespannungszustand in der ideal-plastischen Scheibe*, Ing.-Arch., **36**, 174–191, 1967.
5. P. SÄHN and H. BALKE, *Wärme- und Restspannungen in Kreisringscheiben und ihre Beurteilung*: Parts 1 and 2. Maschinenbautechnik, **18**, 175–182 and 249–254, 1969.
6. H. ODENÖ, *Transient thermal stresses in elasto-plastic discs*, J. Mech. Eng. Sci., **11**, 384–391, 1969.
7. H. ODENÖ, *Transient thermal stresses in discs with a temperature dependent yield stress*, Acta Polyt. Scand. Phys. Incl. Nucleon. Series, No. 66, Stockholm 1969.
8. B. A. BOLEY and J. H. WEINER, *Theory of thermal stresses*, Wiley, New York 1960.
9. P. P. BENHAM and HOYLE [Ed], *Thermal stress*, Pitman, London 1964.

10. A. MENDELSON, *Plasticity. Theory and application*, MacMillan, New York 1968.
11. L. COLLATZ, *Numerische Behandlung von Differentialgleichungen*, Springer, Berlin 1951.
12. H. ODENÖ, *Approximativ lösning av spänningstillståndet i en transient termobelastad cylinder*, intern. rapport nr 176, inst. för hållfasthetslära, Chalmers Univ. Tech., Gothenburg 1969.
13. H. PARKUS, *Instationäre Wärmespannungen*, Springer, Vienna 1959.
14. H. ODENÖ, *Transient thermal stresses in circular discs*, Diss., Chalmers Univ. Tech., Gothenburg 1971.

LINKÖPING UNIVERSITY
DEPARTMENT OF MECHANICAL ENGINEERING
SWEDEN.

Received September 22, 1971.